REVIEW ARTICLE

Assessment of Cardiac Sympathetic Nerve Function Using ^{123}I-meta-Iodobenzylguanidine Scintigraphy: Technical Aspects and Standardization

Shinro Matsuo, MD, PhD, Kenichi Nakajima, MD, PhD

Received: April 21, 2015/Revised manuscript received: May 28, 2015/Accepted: May 28, 2015

Abstract

The ^{123}I-labeled meta-iodobenzylguanidine (MIBG) has been used in clinical medicine since 1992 to assess the severity and prognosis of heart failure. Although values of the heart-to-mediastinum ratio (HMR) were different depending on the difference of scinticamera-collimator systems, the standardization of the HMR became possible by using a calibration phantom. Semi-automated calculation of setting the region of interest for determining the HMR improves the reproducibility of the cardiac and mediastinum regions and might be used in every institution. This article describes standard technical information on techniques of MIBG, including HMR and collimators.

Keywords: Meta-iodobenzylguanidine, Heart-to-mediastinum ratio, Collimator, Standard medium-energy
Ann Nucl Cardiol 2015；1（1）：27-34

The radiolabeled meta-iodobenzylguanidine (MIBG) is a norepinephrine analog that is stored in the myocardium in a similar way to noradrenaline (1). In Japan, the MIBG, as a neurotransmitter agent, has been used in clinical medicine since 1992 (2). ^{123}Iodine labeled MIBG is used for functional assessment of sympathetic innervation of the heart. Japanese Circulation Society guidelines for clinical use of cardiac nuclear medicine documented that MIBG study has class I or IIa evidence for clinical use to assess the severity and prognosis of heart failure (Table 1) (3). MIBG is cleared from the myocardium, but it is not catabolized by monoamine oxidase or catechol-O-methyltransferase. The assessment of MIBG uptake and washout gives us unique information on autonomic nerve function. Distribution of MIBG uptake in the myocardium gives us a much better understanding of the pathophysiology of the disease, including cardiomyopathies, coronary artery disease, diabetes and generalized autonomic neuropathy (4). Despite the prognostic and diagnostic values of MIBG study (5-8), there are still limitations that prevent this technique from being globally used as an essential management tool in a clinical setting (9-10). This article describes standard technical information on techniques of MIBG, including heart-to-mediastinum ratio (HMR) and collimators.

Methods

Acquisition conditions

^{123}I-MIBG, which in Japan is provided by FUJIFILM RI Pharma, Tokyo, has been used for the cardiac studies. ^{123}I-MIBG study requires only minimal pre-test preparation. The consumption of drugs that potentially interfere with catecholamine uptake should be quitted at least 24 hours before the examination. Such drugs include antidepressants, antipsychotics, some calcium channel blockers, inotropic sympathomimetics, β2 stimulants and antiarrhythmics for ventricular arrhythmia (amiodarone) (9). The effects of the necessary

doi：10.17996/ANC. 01. 01. 27

Shinro Matsuo, Kenichi Nakajima
Department of Nuclear Medicine Kanazawa University Hospital,
13-1 Takaramachi, Kanazawa, Ishikawa, Japan 920-8641
E-mail: smatsuo@nmd.m.kanazawa-u.ac.jp

Table 1 Recommendations for myocardial sympathetic nerve imaging using ^{123}I-MIBG

Indications	(1)	(2)
Assessment of severity and prognosis of heart failure	I	B
Assessment of treatment effects of heart failure	II a	C
Arrhythmogenic disease	II b	C

(1): classification of recommendations, (2): level of evidence. ^{123}I-MIBG, ^{123}I-metaiodobenzylguanidine. (adapted from Circ J 2010 76; 763 ref. 3)

Table 2 Comparison of the heart-to-mediastinum ratio among previous articles

Study	Subjects	cut-off values	collimator reference
ADMIRE-HF (6)	HF	1.6	LEHR
MIBG pooled Data in Japan (5)	HF	1.68	LE
Nakata et al. (52)	HF	1.74	LEGP
King (54)	DLB	1.77	LE

ADMIRE-HF, AdreView Myocardial Imaging for Risk Evaluation in Heart Failure; HF, heart failure; DLB, dementia with Lewy bodies; LEHR, low-energy high-resolution; ME, medium energy; LEGP, low-energy general purpose.

withdrawal of the drugs should be evaluated in discussion with the referring physician. Thyroid uptake of free iodide can be prevented using stable iodine administered orally. ^{123}I-MIBG is injected slowly at a typical dose of 111 MBq intravenously at rest. ^{123}I-MIBG planar and single-photon emission computed tomography (SPECT) studies were performed at 20 minutes (early) and 3 hours (delayed) after the injection. The acquisition energy was set 159 keV with a 20% window. Previous prognostic data on MIBG imaging is based on analysis of planar images (11-13).

Imaging

Instrumentation:

A single or multiple head gamma camera with a large field of view is necessary to obtain planar and SPECT images. MIBG images can be obtained using a standard Anger gamma camera, including a dual headed or triple headed camera. Low-energy general-purpose (LEGP) or low-energy high-resolution (LEHR) is commonly applied to collimators because of their wide availability. These collimators are not optimal for ^{123}I study due to thin septa compared to medium energy (ME) type collimators. ME collimators have thicker septa and lower penetration of gamma rays than LE collimators, which have a property of decreasing Compton scatter in scintigraphic images (14-15).

Collimator choice

The European Council of Nuclear Cardiology Committee recommended the use of ME collimators for MIBG images (16). Among many technical factors, collimator choice substantially affects the estimation of HMR. For the conditions of the collimator and camera, the value of HMR obtained from each collimator is different. Even among ME collimators, there is a slight difference in the values of HMR in previous studies (Table 2). A variety of collimators have been used in many countries. We can generally divide all collimators into two categories; LE type and ME type (17-21), and HMR obtained from LE type collimators can be converted into that of ME type (21). The camera venders, however, produced various types of collimators for various purposes of clinical situations. The low-medium energy (LME) collimator is a good example that can cover higher energy scatter portion of ^{123}I energy spectrum, since ^{123}I, including MIBG and BMIPP, are widely used in Japan (21).

The heart-to-mediastinum ratio (HMR), regions of interest (ROI) setting

The HMR has been used to determine the uptake of MIBG in the heart. The HMR is a simple method that allows comparison of inter-individual and inter-institutional results by correcting for differences in body geometry and attenuation between individual subjects. There are several factors that could affect the values of HMR, including the method of ROI setting, choice of collimators, acquisition method, and correction method. Inter-institutional differences of HMR have hampered multi-center comparison of HMR and single-center results could not be extrapolated to other institutions, if

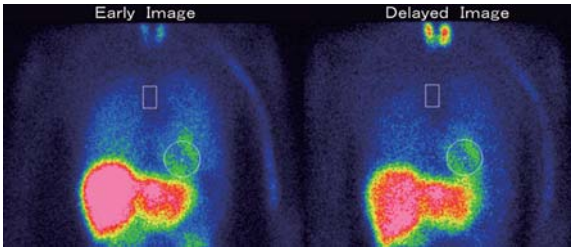

Fig. 1 Semi-quantitative ROI by smartMIBG
The circular ROI in the heart is determined on the cardiac region for evaluating the heart count. The mediastinum midline is set by searching the minimal count on the horizontal chest profile curve.

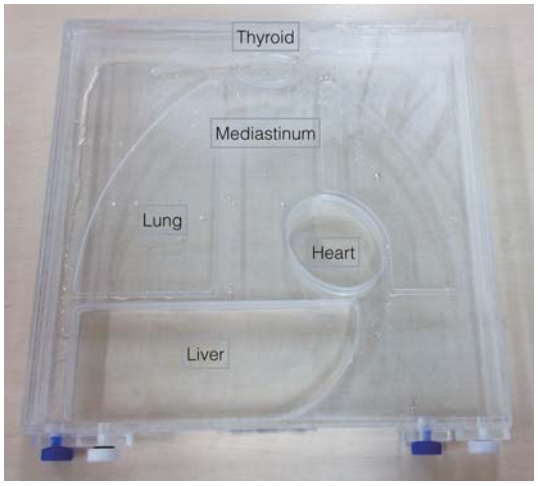

Fig. 2 Calibration phantom Type KB（Hokuiriku Yuuki Industry, Co. Ltd. Kanazawa, Japan）

proper calibration is not used（22-23）. Therefore, these factors should be standardized. Early and delayed HMR can be calculated on the basis of the mean count densities obtained from drawing the ROI of the left ventricle and mediastinum manually or automatically. Many investigators have used manually drawn ROI of the left ventricle and mediastinum in determining the HMR. Visual determination of ROIs for quantitative analysis of MIBG imaging has been a routine nuclear cardiology practice in Japan. Visual definition of the whole-heart ROI and mediastinum is an applicable technique for determining HMR on planar images, which may not result in significant clinical decision change as long as the ROIs are properly placed. Standardization of cardiac and mediastinal ROI setting is one of the most critical aspects for quantitative analysis in ^{123}I-MIBG scintigraphy. Following is a recommended method to determine the ROI. Schematic representation of the ^{123}I-MIBG is shown in Fig. 1, which shows a circular ROI in the heart and rectangular ROI in the mediastinum. As one of the proposed methods, the circular ROI is determined on the cardiac region for evaluating the heart count. In setting a mediastinum ROI, we can use the following method as a reference. The rectangular mediastinal ROI is set in the upper 30% of the lung vertical length and 10% of the horizontal body width. The thyroid and lung should be avoided in setting a mediastinal ROI. By using automated software, the same ROI can be placed even if the analyst is different. The smartMIBG（FUJIFILM RI Pharma Co., Ltd., Tokyo, Japan）software can be used for semi-automated calculation of setting the ROI（24）. Determining the HMR by using the automated method improves the reproducibility of the cardiac ROI and could be used in every institution.

Correction methods

^{123}Iodine has a peak energy emission of 159 keV（97%）. A photopeak window of ^{123}I is centered at 159 keV with a 20% energy window. However, ^{123}I emits high-energy photons, which is a 529 keV component in 1.39% of the total number of photons with its down scatter（25）. These photons may influence the estimation of the HMR causing the underestimation of the values（21）. This scatter photon generally makes the value of HMR lower. The estimated HMR is also potentially affected by acquisition protocol. A scatter correction method called ^{123}I dual-window（IDW）method was proposed（17, 19, 21）. The IDW method proved to be useful in reducing effects of ^{123}I high-energy down-scatter and septal penetration. The difference of collimator becomes an issue when the gamma camera is updated in its own facility. Standardized values of HMR are needed when we compare the data with other facilities, or when multicenter studies are conducted. Therefore, in order to correct the value calculated from the condition difference, the multiple energy window method as triple energy window（TEW）method, as well as IDW method, was proposed（17, 21）. Furthermore, to achieve a simple correction among many institutions, the correction methods based on phantom experiments have been proposed for a standardization of HMR（26-27）. The calibration phantom for ^{123}I-MIBG was made for planar image acquisition, which included heart, lung, mediastinum and liver as shown in Fig. 2. By using the phantom, MIBG HMR measured by an LE collimator can be corrected to ME collimator-comparable values（21）. A phantom experiment based on 225 experiments in 84 institutions all over Japan made it possible to unify all MHR values among various collimators（26）. According to the results of the phantom study（27）, the collimator types might be

Table 3 Differences of transforming coefficients by collimator

Collimator	LE or ME	Conversion coefficient（mean）	SD
LEHR	LE	0.55	0.05
CHR	LE	0.55	0.02
LEGP/AP	LE	0.65	0.04
ELEGP（two groups）	LE	0.62, 0.75	0.03, 0.03
LMEGP	ME	0.83	0.05
MEGP/GAP	ME	0.83	0.05
MELP	ME	0.95	0.04

LEHR, low-energy high-resolution; ME, medium energy; LEGP, low-energy general-purpose. LMEGP, low-medium-energy general-purpose; MEGP, medium-energy general-purpose; LE, low energy; ME, medium energy;

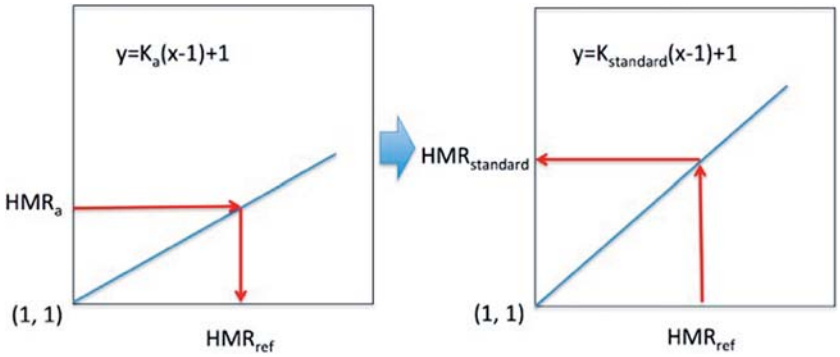

Fig. 3 A Schema of the conversion from institutional heart-to-mediastinum ratio（HMR）to $HMR_{standard}$. Although the conversion is explained in two steps, the calculation can be performed by one equation as shown in the text. $K_{standard}$ of 0.88 is used as the conversion coefficient, which is an average coefficient of common ME collimators.

classified into 7 or 8 major subgroups, although two types, namely LE and ME types, are considered as a rough classification.

A proposal to use standard ME condition

Although we cannot specify one collimator as a standard, we would like to propose to use the average $K_{standard}$ of MEGP collimators as the standard. By phantom experiments, conversion coefficients to the mathematically calculated reference HMR were determined for each camera-collimator system（Table 3）. First, the HMR of a camera A is converted to a theoretical HMR_{ref} by using conversion coefficient of condition A（K_a）, which is the slope of the regression line in the condition. Second, the HMR_{ref} is converted to a standardized HMR（$HMR_{standard}$）using $K_{standard}$（Fig. 3）. The $K_{standard}$ was defined as average K values for typical ME collimators. We can simply calculate it by a formula "$y = K_{standard}/K_a \times (x-1)+1$". Here, as a condition of the collimator standardization, it was decided to make use of K＝0.88, which is the most common ME collimator（standard medium-energy 88, standardME 88）（27）.

The cross-calibration method can be used to apply previous published data to one's own institution. In clinical applications, standardized HMR successfully reclassifies various conditions into the same risk groups of patients.

Washout rate（WR）

WR of MIBG is another value for quantifying MIBG activity and provides information on the sympathetic drive（28-29）. It is preferable to perform background correction and attenuation correction. According to the proposal for cardiac ^{123}I-MIBG guidelines（16）, WR is defined as;

WR（%）＝100x（[(early H count-early M count)-(delayed H count-delayed M count)×k]/(early H count-early M count)

where $k = 1/0.5^{t/13}$（k means time decay correction factor, and t means time in hours）

SPECT image

SPECT can improve the diagnosis of the localization of sympathetic nerve innervation and characterization. Thus SPECT image should be performed when possible. Different types of gamma cameras are available. The characteristics of the camera should be taken into

Table 4 Normal values of heart-to-mediastinum ratio

	Early HMR	Range	Late HMR	Range
LE collimator	2.4	1.9-3.0	2.5	1.9-3.1
ME/LME collimator	2.8	2.0-3.7	3.0	2.0-4.3
Standard ME	3.1	2.2-4.0	3.3	2.2-4.4

HMR, heart-to-mediastinum ratio; LE, low energy; ME, medium-energy; LME, low-medium-energy.

Table 5 Normal values of washout rate

Washout rate	mean 2SD
Time decay correction	16% (6-30)
Time decay and background correction	13% (0-34)

SD, standard deviation.

account to optimize image quality. For SPECT studies, a rotation of 180° or 360° can be used. Images are stored in a 64×64 or 128×128 matrices. The acquisition is comparable to myocardial perfusion imaging.

MIBG distribution of left ventricle

The normal distribution of MIBG in the left ventricular myocardium was not quite homogenous, showing a slight decrease in apex and inferior segments of the left ventricle. A normal Japanese database showed a regional heterogeneity of MIBG uptake, especially in the inferior and apical regions in normal subjects as shown in previous studies (30-32). It has to be kept in mind that MIBG uptake in the inferior wall and in the apex have wide standard deviation and may be decreased in some patients. The decreased uptakes in the apical inferolateral and inferior segment in the delayed images can be seen compared to the initial images (32). The rapid clearance of MIBG in these segments should be remembered in clinical practice, although the real mechanism is unclear. This heterogeneity is considered to be enhanced with the progression of the disease, including heart failure, ischemia, or with age (30-31). The MIBG uptake might vary depending on gender or age. Diabetes may also affect the less inferior uptake of ^{123}I-MIBG (31). Defect score of MIBG can be used to semi-quantify the defect of the left ventricle (31). Regional tracer uptake was assessed semi-quantitatively using a 5-point scoring system (0＝normal to 4＝no uptake) in 17 segments on the delayed SPECT image as recommended in perfusion imaging by the American Heart Association (33). The total defect score (TDS) was calculated as the sum of all defect scores (34). The normal range for the delayed TDS by using an appropriate database is 0-3 (32). However, there is no established SPECT-based method for estimating or scoring MIBG uptake for the patients with heart failure. High activity of liver or lung may be superimposed on myocardial activity in planar images. The inferior wall of the left ventricle might be affected by the high liver uptake (35).

Normal values of HMR and WR, and distribution of SPECT

A normal database was created in Japan as a working group activity of the Japanese Society of Nuclear Medicine (JSNM), and normal values of HMR were shown in Table 4 (32). In the JSNM-working group normal databases ^{123}I-MIBG, average late HMR was 2.5 and 3.0 for LE-collimator and ME-collimator groups. The value of WR is shown in Table 5.

Clinical implication

Early HMR reflects the cardiac sympathetic innervation. Delayed HMR is considered to express the cardiac sympathetic activity, including the number of sympathetic nerve terminals (36-40). The information of distribution of neurons and function of the uptake-1 of MIBG can be obtained by HMR. In a recent ADMIRE-HF study (6), patients with low HMR showed a significantly higher incidence of serious cardiac events including of heart failure and cardiac death. Many clinical studies have recently demonstrated the important role of ^{123}I-MIBG scintigraphy (41-52). MIBG HMR is better than left ventricular ejection fraction for long-term risk stratification (53-55). In part, patients with Lewy-body disease also have low HMR, which reflects a pathological progression of the disease process involving extensive autonomic involvement (54).

Conclusion

The standard technical information on techniques of MIBG, including HMR and collimators, was described in this article. Global abnormality of ^{123}I-MIBG distribution has been reported in various disorders and conditions. The more precisely HMR determined, the more useful the MIBG scintigraphy will be to help health care and

for the patients' managements.

Acknowledgments

We thank Ronald G. Belisle for editorial assistance.

Sources of Funding

This study was supported by JSPS Grants-in-Aid for Scientific Research (C) in Japan (grant number 23591755, PI Shinro Matsuo).

Conflicts of Interest

S. Matsuo and K. Nakajima have a collaborative research work with FUJIFILM RI Pharma, Co. Ltd. Japan, for developing the nuclear cardiology software.

No other potential conflict of interest relevant to this article was reported.

Reprint requsts and correspondence：

Shinro Matsuo,

Department of Nuclear Medicine Kanazawa University Hospital, 13-1 Takaramachi, Kanazawa, Ishikawa, Japan 920-8641

E-mail: smatsuo@nmd.m.kanazawa-u.ac.jp

References

1. Carrio I. Cardiac neurotransmission imaging. J Nucl Med 2001; 42: 1062-76.
2. Yamashina S, Yamazaki J. Neuronal imaging using SPECT. Eur J Nucl Med Mol Imaging 2007; 34: 939-50.
3. Tamaki N, Kumita S, Kusakabe K, et al. Guidelines for clinical use of cardiac nuclear medicine (JCS 2010)-digest version-. Circ J 2012; 76: 761-7.
4. Matsuo S, Nakajima K, Kinuya S. Clinical use of nuclear cardiology in the assessment of heart failure. World J Cardiol 2010; 2: 344-56.
5. Nakata T, Nakajima K, Yamashina S, et al. A pooled analysis of multicenter cohort studies of ^{123}I-mIBG imaging of sympathetic innervation for assessment of long-term prognosis in heart failure. JACC Cardiovasc Imaging 2013; 6: 772-84.
6. Jacobson AF, Senior R, Cerqueira MD, et al. Myocardial iodine-123 metaiodobenzylguanidine imaging and cardiac events in heart failure. Results of the prospective ADMIRE-HF (AdreView Myocardial Imaging for Risk Evaluation in Heart Failure) study. J Am Coll Cardiol 2010; 55: 2212-21.
7. Kuramoto Y, Yamada T, Tamaki S, et al. Usefulness of cardiac iodine-123 meta-iodobenzylguanidine imaging to improve prognostic power of Seattle heart failure model in patients with chronic heart failure. Am J Cardiol 2011; 107: 1185-90.
8. Kuwabara Y, Tamaki N, Nakata T, Yamashina S, Yamazaki J. Determination of the survival rate in patients with congestive heart failure stratified by ^{123}I-MIBG imaging: a metaanalysis from the studies performed in Japan. Ann Nucl Med 2011; 25: 101-7.
9. Tamaki N, Kuge Y, Yoshinaga K. Molecular imaging in heart failure patients. Clin Transl Imaging 2013; 1: 341-51.
10. Agostini D, Verberne HJ, Burchert W, et al. ^{123}I-mIBG myocardial imaging for assessment of risk for a major cardiac event in heart failure patients: insights from a retrospective European multi-center study. Eur J Nucl Med Mol Imaging 2008; 35: 535-46.
11. Takeishi Y, Atsumi H, Fujiwara S, Takahashi K, Tomoike H. ACE inhibition reduces cardiac iodine-123-MIBG release in heart failure. J Nucl Med 1997; 38: 1085-9.
12. Toyama T, Aihara Y, Iwasaki T, et al. Cardiac sympathetic activity estimated by ^{123}I-MIBG myocardial imaging in patients with dilated cardiomyopathy after beta-blocker or angiotensin-converting enzyme inhibitor therapy. J Nucl Med 1999; 40: 217-23.
13. Kasama S, Toyama T, Sumino H, et al. Prognostic value of serial cardiac ^{123}I-MIBG imaging in patients with stabilized chronic heart failure and reduced left ventricular ejection fraction. J Nucl Med 2008; 49: 907-14.
14. Verberne HJ, Feenstra C, de Jong WM, Somsen GA, van Eck-Smit BL, Busemann Sokole E. Influence of collimator choice and simulated clinical conditions on ^{123}I-MIBG heart/mediastinum ratios: a phantom study. Eur J Nucl Med Mol Imaging 2005; 32: 1100-7.
15. Inoue Y, Suzuki A, Shirouzu I, et al. Effect of collimator choice on quantitative assessment of cardiac iodine 123 MIBG uptake. J Nucl Cardiol 2003; 10: 623-32.
16. Flotats A1, Carrió I, Agostini D, et al. Proposal for standardization of ^{123}I-metaiodobenzylguanidine (MIBG) cardiac sympathetic imaging by the EANM Cardiovascular Committee and the European Council of Nuclear Cardiology. Eur J Nucl Med Mol Imaging 2010; 37: 1802-12.
17. Motomura N, Ichihara T, Takayama T, Aoki S, Kubo H, Takeda K. Practical compensation method of downscattered component due to high energy photon in ^{123}I imaging. Kaku Igaku 1999; 36: 997-1005.
18. Inoue Y, Abe Y, Asano Y, Kikuchi K, Iizuka T, Nishiyama K. Septal penetration in iodine-123 metaiodobenzylguanidine cardiac sympathetic imaging using a medium-energy collimator. J Nucl Cardiol 2014; 21: 71-7.
19. Nakajima K, Matsubara K, Ishikawa T, et al. Correction of I-123-labeled meta-iodobenzylguanidine uptake with multi-window methods for standardization of the heart to mediastinum ratio. J Nucl Cardiol 2007; 14: 843-51.
20. Inoue Y, Abe Y, Itoh Y, et al. Acquisition protocols and correction methods for estimation of the heart- to-mediastinum ratio in ^{123}I-metaiodobenzylguanidine cardiac sympathetic imaging. J Nucl Med 2013; 54: 707-13.

21. Matsuo S, Nakajima K, Okuda K, et al. Standardization of the heart-to-mediastinum ratio of iodine-123-labeled-meta-iodobenzylguanidine uptake using dual energy window method: Feasibility of correction from different camera-collimator combinations. Eur J Nucl Med Mol Imaging 2009; 36: 560-6.
22. Slomka PJ, Mehta PK, Germano G, Berman DS. Quantification of I-123-meta-iodobenzylguanidine heart-to-mediastinum ratios: Not so simple after all. J Nucl Cardiol 2014; 21: 979-83.
23. Jacobson AF, Matsuoka DT. Influence of myocardial region of interest definition on quantitative analysis of planar ^{123}I-mIBGimages. Eur J Nucl Med Mol Imaging 2013; 40: 558-64.
24. Okuda K, Nakajima K, Hosoya T, et al. Semi-automated algorithm for calculating heart-to-mediastinum ratio in cardiac Iodine-123 MIBG imaging. J Nucl Cardiol 2011; 18: 82-9.
25. Kobayashi H, Momose M, Kanaya S, Kondo C, Kusakabe K, Mitsuhashi N. Scatter correction by two-window method standardizes cardiac I-123 MIBG uptake in various gamma camera systems. Ann Nucl Med 2003; 17: 309-13.
26. Nakajima K, Okuda K, Matsuo S, et al. Standardization of metaiodobenzylguanidine heart to mediastinum ratio using a calibration phantom: effects of correction on normal databases and a multi-center study. Eur J Nucl Med Mol Imaging 2012; 39: 113-9.
27. Nakajima K, Okuda K, Yoshimura M, et al. Multicenter cross-calibration of I-123 metaiodobenzylguanidine heart-to-mediastinum ratios to overcome camera-collimator variation. J Nucl Cardiol 2014; 21: 970-8.
28. Yamada T, Shimonagata T, Fukunami M, et al. Comparison of the prognostic value of cardiac iodine-123 metaiodobenzylguanidine imaging and heart rate variability in patients with chronic heart failure: a prospective study. J Am Coll Cardiol 2009; 41: 231-8.
29. van der Veen BJ, Al Younis I, de Roos A, Stokkel MP. Assessment of global cardiac I-123 MIBG uptake and washout using volumetric quantification of SPECT acquisitions. J Nucl Cardiol 2012; 19: 752-62.
30. Tsuchimochi S, Tamaki N, Tadamura E, et al. Age and gender differences in normal myocardial adrenergic neuronal function evaluated by iodine-123-MIBG imaging. J Nucl Med 1995; 36: 969-74.
31. Matsuo S, Takahashi M, Nakamura Y, Kinoshita M. Evaluation of cardiac sympathetic innervation with iodine-123-metaiodobenzylguanidine imaging in silent myocardial ischemia. J Nucl Med 1996; 37: 712-7.
32. Matsuo S, Nakajima K, Yamashina S, et al. Characterization of Japanese standards for myocardial sympathetic and metabolic imaging in comparison with perfusion imaging. Ann Nucl Med 2009; 23: 517-22.
33. Cerqueira MD, Weissman NJ, Dilsizian V, et al. Standardized myocardial segmentation and no-menclature for tomographic imaging of the heart. A statement for healthcare professionals from the Cardiac Imaging Committee of the Council on Clinical Cardiology of the American Heart Association. Circulation 2002; 105: 539-42.
34. Kasama S, Toyama T, Funada R, et al. Effects of adding intravenous nicorandil to standard therapy on cardiac sympathetic nerve activity and myocyte dysfunction in patients with acute decompensated heart failure. Eur J Nucl Med Mol Imaging 2015; 42: 761-70.
35. Verschure DO, de Wit TC, Bongers V, et al. ^{123}I-MIBG heart-to-mediastinum ratio is influenced by high-energy photon penetration of collimator septa from liver and lung activity. Nucl Med Commun 2015; 36: 279-85.
36. Matsuo S, Nakamura Y, Takahashi M, et al. Cardiac sympathetic dysfunction in athlete's heart detected by ^{123}I-MIBG scintigraphy. Jpn Circ J 2001; 65: 371-4.
37. Matsuo S, Nakamura Y, Tsutamoto T, Kinoshita M. Impairments of myocardial sympathetic activity may reflect the progression of myocardial damage or dysfunction in hypertrophic cardiomyopathy. J Nucl Cardiol 2002; 9; 407-12.
38. Matsuo S, Nakamura Y, Matsumoto T, et al. Prognostic value of iodine-123 metaiodobenzylguanidine imaging in patients with heart failure. Exp Clin Cardiol 2003; 8: 95-8.
39. Horiguchi Y, Morita Y, Tsurikisawa N, Akiyama K. ^{123}I-MIBG imaging detects cardiac involvement and predicts cardiac events in Churg-Strauss syndrome. Eur J Nucl Med Mol Imaging 2011; 38: 221-9.
40. Katoh S, Shishido T, Kutsuzawa D, et al. Iodine-123-metaiodobenzylguanidine imaging can predict future cardiac events in heart failure patients with preserved ejection fraction. Ann Nucl Med 2010 ; 24: 679-86.
41. Nishisato K, Hashimoto A, Nakata T, et al. Impaired cardiac sympathetic innervation and myocardial perfusion are related to lethal arrhythmia: quantification of cardiac tracers in patients with ICDs. J Nucl Med 2010; 51: 1241-9.
42. Honda Y, Toyama T, Miyaishi Y, et al. Combination of ^{123}I-metaiodobenzylguanidine scintigraphy and flow-mediated dilation for the detection of patients with coronary spastic angina. J Nucl Cardiol 2014; 21: 643-51.
43. Akutsu Y, Kaneko K, Kodama Y, et al. Usefulness of severe cardiac sympathetic dysfunction to predict the occurrence of rapid atrial fibrillation in patients with Wolff-Parkinson-White syndrome. Am J Cardiol 2013; 112: 688-93.
44. Yonezawa M, Nagao M, Abe K, et al. Relationship between impaired cardiac sympathetic activity and spatial dyssynchrony in patients with non-ischemic heart failure: assessment by MIBG scintigraphy and tagged MRI. J Nucl Cardiol 2013; 20: 600-8.
45. Murozono Y, Yufu K, Takahashi N, et al. Combined assessment of baroreflex sensitivity with iodine 123 metaiodobenzylguanidine scintigraphic findings strengthens the power of predictive value for cerebral and

cardiovascular events in type 2 diabetic patients. Circ J 2013 ; 77: 130–6.
46. Koyama T, Watanabe H, Tamura Y, Oguma Y, Kosaka T, Ito H. Adaptive servo-ventilation therapy improves cardiac sympathetic nerve activity in patients with heart failure. Eur J Heart Fail 2013; 15: 902–9.
47. Yoshinaga K, Tomiyama Y, Manabe O, et al. Prone-position acquisition of myocardial ^{123}I-metaiodobenzylguanidine（MIBG）SPECT reveals regional uptake similar to that found using（11）C-hydroxyephedrine PET/CT. Ann Nucl Med 2014; 28: 761–9.
48. Matsunari I, Aoki H, Nomura Y, et al. Iodine-123 metaiodobenzylguanidine imaging and carbon-11 hydroxyephedrine positron emission tomography compared in patients with left ventricular dysfunction. Circ Cardiovasc Imaging 2010; 3: 595–603.
49. Tamaki S, Yamada T, Okuyama Y, et al. Cardiac iodine-123 metaiodobenzylguanidine imaging predicts sudden cardiac death independently of left ventricular ejection fraction in patients with chronic heart failure and left ventricular systolic dysfunction: results from a comparative study with signal-averaged electrocardiogram, heart rate variability, and QT dispersion. J Am Coll Cardiol 2009; 53: 426–35.
50. Matsuo S, Nakajima K, Akhter N, Okuda K, Kinuya S. Diagnostic and prognostic cardiac imaging in cardiomyopathies. Cardiomyopathies: Causes, Effects and Treatment. NOVA publishers 2009, p.p.35–43.
51. Matsuo S, Nakamura Y, Matsui T, Matsumoto T, Kinoshita M. Detection of denervated but viable myocardium in cardiac sarcoidosis with I-123 MIBG and Tl-201 SPECT Imaging. Ann Nucl Med 2001; 15: 373–5.
52. Nakata T, Miyamoto K, Doi A, et al. Cardiac death prediction and impaired cardiac sympathetic innervation assessed by MIBG in patients with failing and nonfailing hearts. J Nucl Cardiol 1998; 5: 579–90.
53. Matsuo S, Nakae I, Masuda D, Matsumoto T, Horie M. Dilated cardiomyopathy relieved as a result of beta-blocker therapy: a case report--key points in assessment of prognosis based on MIBG myocardial scintigraphy and BNP levels. Ann Nucl Med 2005; 19: 243–6.
54. King AE, Mintz J, Royall DR. Meta-analysis of ^{123}I-MIBG cardiac scintigraphy for the diagnosis of Lewy body-related disorders. Mov Disord 2011; 26: 1218–24.
55. Matsuo S, Nakajima K, Nakata T, et al. Prognostic values of cardiac sympathetic imaging in heart failure patients: a difference between ischemic and non-ischemic etiologies. J Nucl Med 2014; 55: 17245.